AMERICAN SOCIETY FOR MICROBIOLOGY | mBio®

RESEARCH ARTICLE
Host-Microbe Biology

A Novel *Enterococcus faecalis* Heme Transport Regulator (FhtR) Senses Host Heme To Control Its Intracellular Homeostasis

Vincent Saillant,[a] Damien Lipuma,[a] Emeline Ostyn,[a] Laetitia Joubert,[a]* Alain Boussac,[b] Hugo Guerin,[a] Géraldine Brandelet,[c] Pascal Arnoux,[c] Delphine Lechardeur[a]

[a]Micalis Institute, INRAE, AgroParisTech, Université Paris-Saclay, Jouy-en-Josas, France
[b]I2BC, CNRS UMR 9198, CEA Saclay, Gif-sur-Yvette, France
[c]Aix Marseille Université, CEA, CNRS, BIAM, Saint Paul-Lez-Durance, France

ABSTRACT *Enterococcus faecalis* is a commensal Gram-positive pathogen found in the intestines of mammals and is also a leading cause of severe infections occurring mainly among antibiotic-treated dysbiotic hospitalized patients. Like most intestinal bacteria, *E. faecalis* does not synthesize heme (in this report, heme refers to iron protoporphyrin IX regardless of the iron redox state). Nevertheless, environmental heme can improve *E. faecalis* fitness by activating respiration metabolism and a catalase that limits hydrogen peroxide stress. Since free heme also generates toxicity, its intracellular levels need to be strictly controlled. Here, we describe a unique transcriptional regulator, FhtR (named FhtR for faecalis heme transport regulator), which manages heme homeostasis by controlling an HrtBA-like efflux pump (named $HrtBA_{Ef}$ for the HrtBA from *E. faecalis*). We show that FhtR, by managing intracellular heme concentration, regulates the functional expression of the heme-dependent catalase A (KatA), thus participating in heme detoxification. The biochemical features of FhtR binding to DNA, and its interaction with heme that induces efflux, are characterized. The FhtR-$HrtBA_{Ef}$ system is shown to be relevant in a mouse intestinal model. We further show that FhtR senses heme from blood and hemoglobin but also from cross-feeding by *Escherichia coli*. These findings bring to light the central role of heme sensing by FhtR in response to heme fluctuations within the gastrointestinal tract, which allow this pathogen to limit heme toxicity while ensuring expression of an oxidative defense system.

IMPORTANCE *Enterococcus faecalis*, a normal and harmless colonizer of the human intestinal flora can cause severe infectious diseases in immunocompromised patients, particularly those that have been heavily treated with antibiotics. Therefore, it is important to understand the factors that promote its resistance and its virulence. *E. faecalis*, which cannot synthesize heme, an essential but toxic metabolite, needs to scavenge this molecule from the host to respire and fight stress generated by oxidants. Here, we report a new mechanism used by *E. faecalis* to sense heme and trigger the synthesis of a heme efflux pump that balances the amount of heme inside the bacteria. We show in a mouse model that *E. faecalis* uses this mechanisms within the gastrointestinal tract.

KEYWORDS *Enterococcus faecalis*, heme homeostasis, heme transport, microbiota, stress adaptation, transcriptional regulation

Enterococcus faecalis is a commensal inhabitant of the gastrointestinal tract (GIT) and a subdominant species in the core intestinal microbiota of healthy humans and other mammals (1). This lactic acid bacterium is also a major opportunistic pathogen that causes a large number of nosocomial infections such as endocarditis, bacteremia, urinary tract infections, or meningitis (2). In recent decades, *E. faecalis* has emerged

Citation Saillant V, Lipuma D, Ostyn E, Joubert L, Boussac A, Guerin H, Brandelet G, Arnoux P, Lechardeur D. 2021. A novel *Enterococcus faecalis* heme transport regulator (FhtR) senses host heme to control its intracellular homeostasis. mBio 12:e03392-20. https://doi.org/10.1128/mBio.03392-20.

Editor Gary M. Dunny, University of Minnesota Medical School

Copyright © 2021 Saillant et al. This is an open-access article distributed under the terms of the Creative Commons Attribution 4.0 International license.

Address correspondence to Delphine Lechardeur, delphine.lechardeur@inrae.fr.

* Present address: Laetitia Joubert, Abolis Biotechnologies, Evry, France.

Received 3 December 2020
Accepted 7 December 2020
Published 2 February 2021

as a leading cause of enterococcal infections, and it is the third most frequent source of hospital-acquired nosocomial infections (3). *E. faecalis* is thus considered a major public health threat due to its intrinsic resistance to antibiotics and the emergence of multidrug-resistant isolates (3). Selective outgrowth of enterococci following intestinal dysbiosis is frequent, regardless of whether it results from antibiotic treatment, intestinal inflammation, or infection (4). In addition to intrinsic and acquired antibiotic resistances, *E. faecalis* is resistant to other antimicrobial factors, such as bile, and tolerates a wide variety of stress factors such as temperature, pH, oxygen tension, or oxidation (1).

For most living organisms, heme (iron porphyrin) (in this report, heme refers to iron protoporphyrin IX regardless of the iron redox state, whereas hemin refers to ferric iron protoporphyrin IX) is an essential cofactor of enzymes such as cytochromes, catalases, or peroxidases (5). The importance of heme resides in the unique properties of its iron center, including the capacity to undergo electron transfer, to perform acid-base reactions and to interact with various coordinating ligands (6). Paradoxically, the high potential redox of heme iron catalyzes the production of reactive oxygen species (ROS). Oxidative stress generated by heme together with its accumulation in membranes explains its toxicity (7–9). Most bacteria carry the enzymatic machinery for endogenous heme synthesis. However, numerous bacteria lack some or all the enzymes needed for autosynthesis but still require this molecule for their metabolism (5). Interestingly, *E. faecalis*, like the majority of species constituting the ga`strointestinal microbiota, cannot synthesize heme (10, 11). When heme is added to an aerated culture, *E. faecalis* activates a terminal cytochrome *bd* oxidase, causing a shift from fermentation to an energetically favorable respiratory metabolism (11, 12). *E. faecalis*, unlike other *Firmicutes* that cannot synthesize heme, also carries a gene that encodes a heme catalase (KatA; EC 1.11.1.6), limiting hydrogen peroxide stress when heme is available (10). Both activities contribute to the virulence of several Gram-positive pathogens (13, 14). Although the importance of heme as a cofactor for numerous cellular functions is established (5, 15), the mechanisms governing exogenous heme internalization and secretion that contribute to heme homeostasis vary among bacteria and are poorly understood. However, heme homeostasis must be strictly regulated in all bacteria to avoid toxicity (6, 8). Heme efflux is a documented defense mechanism against heme toxicity in some *Firmicutes*. (i) The Pef regulon comprises two multidrug resistance efflux pumps and a MarR-type heme-responsive regulator in *Streptococcus agalactiae* (16). (ii) The HatRT system involves a TetR family heme binding transcriptional regulator (HatR) and a major facilitator superfamily heme transporter (HatT) in *Clostridium difficile* (17). (iii) Heme homeostasis in several Gram-positive bacteria relies on HrtBA (heme-regulated transport) proteins, an ABC transporter, which promotes heme efflux (14, 18–20). Expression of *hrtBA* is controlled by *hssRS* genes, encoding a two-component heme sensor and response regulator in numerous Gram-positive pathogens, including *S. agalactiae*, *Staphylococcus aureus*, and *Bacillus anthracis* (14, 19–22). In contrast, the food bacterium *Lactococcus lactis* regulates HrtBA expression via the TetR family heme sensor HrtR (19). To date, the mechanisms involved in *E. faecalis* management of environmental heme are unknown.

In this work, we describe the mechanism by which a novel *E. faecalis* TetR regulator, called FhtR (for faecalis heme transport regulator), induces expression of $HrtBA_{Ef}$ (named $HrtBA_{Ef}$ for the HrtBA from *E. faecalis*), a conserved heme efflux transporter. We show that FhtR binds intracellular heme, resulting in derepression and increased transcription of $hrtBA_{Ef}$. Heme iron coordination specifies FhtR as a heme sensor, and a critical role for the tyrosine 132 was defined. Our results also establish this system as a master mechanism of control of intracellular heme availability as shown by its requirement for the expression of the heme-dependent *E. faecalis* KatA. Finally, the relevance of the FhtR system to *E. faecalis* is shown in a mouse intestine model, suggesting the importance of FhtR for *E. faecalis* adaptation in the GIT. Our conclusions lead to a new picture of heme homeostasis in *E. faecalis*.

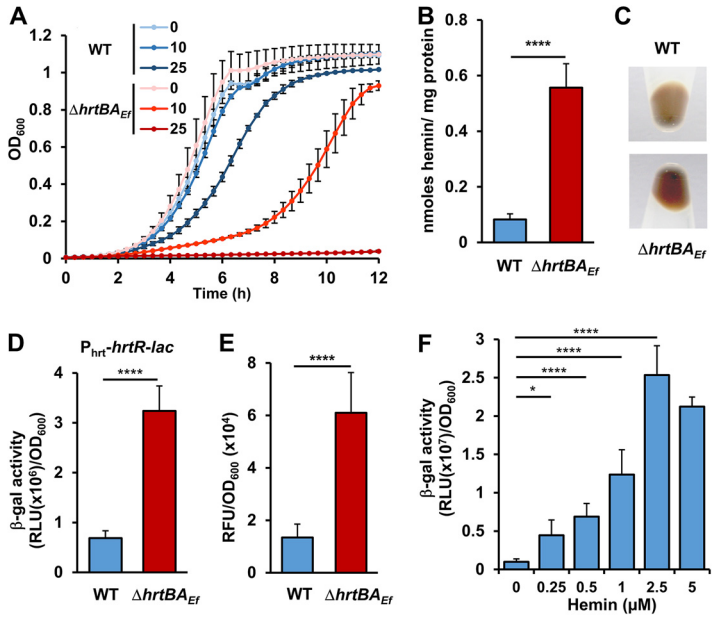

FIG 1 HrtBA$_{Ef}$ controls and responds to heme intracellular concentration. (A) Deletion of *hrtBA*$_{Ef}$ increases sensitivity to hemin toxicity. Overnight cultures of WT and Δ*hrtBA*$_{Ef}$ strains were diluted to an OD_{600} of 0.01 and grown with the indicated concentrations of hemin (in micromolar) for 10 h at 37°C in a microplate Spark spectrophotometer (Tecan). OD_{600} was measured every 20 min. Values are the means ± standard deviations (error bars) from three biological replicates. (B) Heme accumulates in the Δ*hrtBA*$_{Ef}$ strain. WT and Δ*hrtBA*$_{Ef}$ strains were grown to an OD_{600} of 0.5 prior to the addition of 5 μM hemin in the culture medium for an additional 1.5 h. Bacteria were pelleted by centrifugation, and heme content was determined by the pyridine hemochrome assay on cell lysates. Heme content was normalized to the protein concentration. Background from bacteria not incubated with hemin was subtracted. Results represent the means plus standard deviations (error bars) from three biological replicates. Statistical significance was determined by *t* test where **** = $P < 0.0001$. (C) Visualization of cellular heme accumulation in the Δ*hrtBA*$_{Ef}$ mutant. Cells, grown as described above for panel A, were incubated for 1.5 h with 5 μM hemin. The bacteria were photographed following centrifugation. The results are representative of three independent experiments. (D) HrtBA$_{Ef}$ reduces heme cytoplasmic concentration. WT and Δ*hrtBA*$_{Ef}$ strains carrying the intracellular sensor plasmid, pP_{hrt}-*hrtR-lac* were grown as described above for panel B. β-Gal activity was quantified by luminescence in relative light units [RLU]) after 1.5 h of incubation with 5 μM hemin. Results represent the means plus standard deviations from three biological replicates. Statistical significance was determined by *t* test where **** = $P < 0.0001$. (E) HrtBA$_{Ef}$ prevents hemin-induced oxidative stress. WT and Δ*hrtBA*$_{Ef}$ strains were grown as described above for panel B with 5 μM hemin. Cells were washed with PBS plus 0.5% glucose, and ROS generation was quantified by the fluorescence of dihydrorhodamine 123. Results represent the means plus standard deviations from three biological replicates. Fluorescence background from bacteria not incubated with hemin was subtracted. Statistical significance was determined by *t* test where **** = $P < 0.0001$. (F) Induction of *hrtBA*$_{Ef}$ operon by hemin. The WT strain transformed with the reporter plasmid pP_{hrtBA}-*lac* was grown, and β-gal activity was determined as described above for panel D following incubation with the indicated concentrations of hemin. Results represent the means ± standard deviations from three biological replicates. Statistical significance was determined by one-way analysis of variance (ANOVA) with Dunnett's multiple-comparison test comparing each concentration of hemin to no-hemin control with statistical significance indicated as follows: *, $P = 0.0202$; ****, $P < 0.0001$.

RESULTS

The conserved heme efflux transporter HrtBA$_{Ef}$ is functional in *E. faecalis*. *E. faecalis* OG1RF genome encodes two adjacent open reading frames (ORFs), OG1RF_RS02770 and OG1RF_RS02775 sharing, respectively 24% and 45% amino acid (AA) sequence identity with HrtB and HrtA from *Staphylococcus aureus* (18) (see Fig. S1A and S1B in the supplemental material). We thus verified the role of these ORFs, referred to as HrtB$_{Ef}$ and HrtA$_{Ef}$, in heme efflux. Growth of an in-frame Δ*hrtBA*$_{Ef}$ deletion mutant was severely impaired at hemin concentrations $\geq$ 25 μM compared to the wild-type (WT) OG1RF strain (Fig. 1A). However, WT OG1RF could overcome up to 500 μM hemin, highlighting the involvement of HrtBA$_{Ef}$ in limiting heme toxicity in *E. faecalis*

(Fig. S1C). The Δ*hrtBA*$_{Ef}$ mutant grown in 5 μM heme-containing medium accumulated about twofold more intracellular heme than the WT strain, as evaluated by the pyridine hemochrome assay (23) (Fig. 1B). This result correlated with the intense red color of culture pellets from the Δ*hrtBA*$_{Ef}$ mutant compared to the WT strain (Fig. 1C). Intracellular heme concentrations were also monitored using the intracytoplasmic heme sensor HrtR (19): β-galactosidase (β-gal) activity from the reporter plasmid P$_{hrt}$-*hrtR-lac* was about 4 times higher in Δ*hrtBA*$_{Ef}$ compared to the WT exposed to 5 μM heme (Fig. 1D). Finally, accumulation of heme in the Δ*hrtBA*$_{Ef}$ mutant correlated with a more than twofold increase of cellular ROS generated by heme as shown by the fluorescence of dihydrorhodamine 123 (24) (Fig. 1E). In conclusion, *E. faecalis* expresses a functional HrtBA$_{Ef}$ heme efflux transporter that modulates intracellular heme levels, thus reducing oxidative stress.

Transcriptional regulation of *hrtBA*$_{Ef}$ by heme was then investigated using a *hrtBA*$_{Ef}$ promoter reporter, P$_{hrtBA}$-*lac*. β-Gal expression in the WT strain was induced as a function of concentration between 0.1 and 2.5 μM hemin in the culture medium. Induction reached a maximum at concentrations below 5 μM (Fig. 1F). This concentration range is far below WT strain sensitivity to heme toxicity ($\geq$25 μM) (Fig. 1A). We conclude that HrtBA$_{Ef}$ expression is induced at subtoxic heme concentrations.

A new TetR regulator, FhtR, controls *hrtBA*$_{Ef}$ expression. The above findings prompted us to investigate the mechanism of *hrtBA*$_{Ef}$ induction. Several Gram-positive pathogens regulate *hrtBA*$_{Ef}$ via an adjacent two-component system HssR and HssS (14, 20, 21). No *hssR hssS* genes were identified in or near the *hrtBA*$_{Ef}$ operon in *E. faecalis* OG1RF or other *E. faecalis* genomes. However, a monocistronic gene encoding a TetR family transcriptional regulator, OG1RF_RS02765, is adjacent to *hrtBA*$_{Ef}$ (Fig. 2A), sharing no significant AA identity with the *hrtBA* regulator, HrtR, in *Lactococcus lactis* (19). We hypothesized that OG1RF_RS02765 was the transcriptional regulator of *hrtBA*$_{Ef}$ and tentatively named it FhtR (for faecalis heme transport regulator) (Fig. 2A).

To investigate the role of FhtR in heme-dependent transcription of *hrtBA*$_{Ef}$, an *fhtR* in-frame deletion in strain OG1RF (Δ*fhtR*) was constructed and transformed either with pP$_{hrtBA}$-*lac* or p*fhtR* encompassing both (pP$_{hrtBA}$-*lac* and P$_{fhtR}$-*fhtR*) expression cassettes (Fig. 2B). In contrast to the WT strain, β-gal was expressed independently of heme in Δ*fhtR*(pP$_{hrtBA}$-*lac*) (Fig. 2B). Transformation of p*fhtR* with Δ*fhtR* led to overcomplementation compared to the WT(pP$_{hrtBA}$-*lac*) strain (Fig. 2B). Moreover, on solid medium, Δ*fhtR* exhibited a complete absence of sensitivity to heme compared to the WT and complemented Δ*fhtR*(p*fhtR*) strains (Fig. 2C). Similar results were obtained in liquid culture (Fig. S2). These results are in line with the observation that heme accumulation is reduced in the Δ*fhtR* mutant strain compared to the WT or Δ*fhtR*(p*fhtR*) strain (Fig. 2D) and that HrtBA$_{Ef}$ may be constitutively expressed in the Δ*fhtR* mutant (Fig. 2B). Indeed, P$_{fhtR}$ was constitutively transcribed, with no effects of heme, nor of FhtR expression as shown using P$_{fhtR}$-*lac* as the reporter (Fig. 2E), and by Western blotting (WB) using FhtR-hemagglutinin (HA) tagged fusion expressed from P$_{fhtR}$ (Fig. 2F). We conclude that *E. faecalis* uses a constitutively expressed, unique intracellular heme sensor, FhtR, to control *hrtBA*$_{Ef}$ expression.

FhtR is a heme binding protein. Members of the TetR family of transcriptional regulators act as chemical sensors (25, 26). Ligand binding alleviates TetR protein interactions with their respective operators, leading to promoter induction (25, 26). To verify that heme was the signal that relieves FhtR-mediated *hrtBA*$_{Ef}$ repression, recombinant FhtR was purified as a fusion to the maltose binding protein (MBP-FhtR) from *Escherichia coli*. MBP-FhtR appeared green (Fig. 3A, inset), and its UV-visible spectrum exhibited a strong Soret band, suggesting that FhtR scavenges endogenously produced heme (Fig. 3A). To purify an apoFhtR, MBP-FhtR was expressed from a heme synthesis-deficient *E. coli* strain (*hemA*::*kan*) (Fig. 3B, dashed line). The purified protein bound hemin *b in vitro* (i.e., noncovalently) with a similar UV-visible spectrum as observed above for *in vivo*-bound heme: a Soret band at 407 nm and Q bands at 491 nm, 528 nm, and 608 nm (Fig. 3B, holoFhtR). Size-exclusion chromatography profiles showed that both apo- and holo-MBP-FhtR eluted as a single peak corresponding

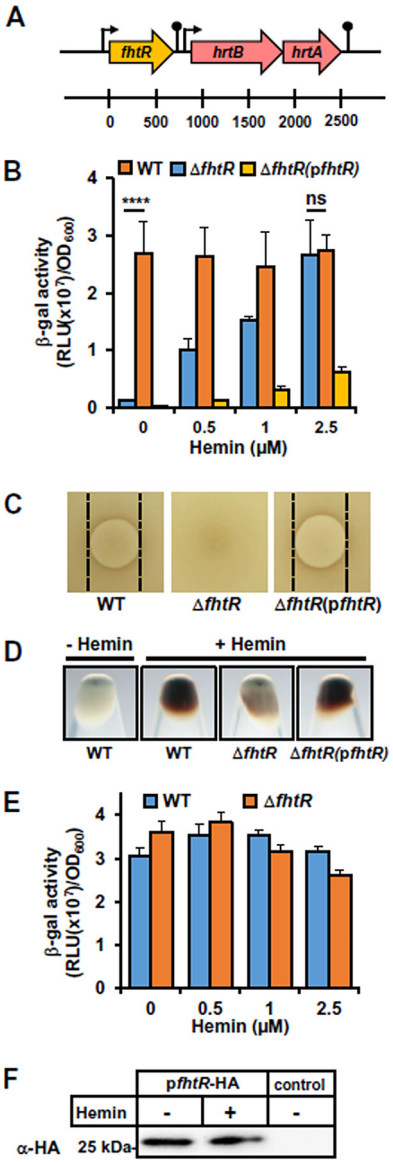

FIG 2 FhtR controls $hrtBA_{Ef}$ expression. (A) Schematic representation of the *fhtR* gene and $hrtBA_{Ef}$ operon. The *fhtR* gene (OG1RF_RS02765) encodes a TetR family transcriptional regulator. The $hrtB_{Ef}$ (OG1RF_RS02770) and $hrtA_{Ef}$ (OG1RF_RS02775) genes encode a permease and ATPase, respectively. (B) FhtR controls $hrtBA_{Ef}$ expression. WT and Δ*fhtR* strains carrying the reporter plasmid pP_{hrtBA}-*lac* and a Δ*fhtR* strain carrying a plasmid, p*fhtR*, combining both P_{hrtBA}-*lac* and P_{fhtR}-*fhtR* were grown to an OD_{600} of 0.5, and β-gal expression was quantified by luminescence as reported in the legend to Fig. 1 with the indicated concentrations of hemin. Results represent the means plus standard deviations (error bars) from three biological replicates. Statistical significance was determined by *t* test as follows: ns, not significant ($P > 0.5$); ****, $P < 0.0001$. (C) *fhtR* deletion abrogates heme toxicity. Stationary-phase cultures of WT, Δ*fhtR*, and Δ*fhtR*(p*fhtR*) strains were plated on solid medium. Hemin (10 μl of a 1 mM stock solution) was pipetted directly onto plates, which were incubated for 24 h. Inhibition zones appear as a circular clearing in the center of each panel. No inhibition zone was observed for the Δ*fhtR* strain. The results are representative of three independent experiments. (D) Visualization of the impact of FhtR on heme accumulation. WT, Δ*fhtR*, and Δ*fhtR*(p*fhtR*) strains were grown and incubated with 5 μM hemin as described above for panel A. The bacteria were pelleted by centrifugation and photographed. The results are representative of three independent experiments. (E) FhtR expression is constitutively induced. β-Gal expression upon hemin addition to the culture medium in WT and Δ*fhtR* strains transformed with the pP_{fhtR}-*lac* reporter plasmid was determined by luminescence as described in the legend to Fig. 1. Results represent the means plus standard deviations from three biological replicates. (F) *fhtR* transcription is not mediated by hemin. The Δ*fhtR* strain transformed with pP_{fhtR}-*fhtR*-HA or carrying an empty vector (control) was used to monitor FhtR expression by Western blotting (WB) using an antihemagglutinin (anti-HA) antibody (α-HA). Bacteria were grown to an OD_{600} of 0.5 and incubated with 2.5 μM hemin for 1.5 h. Sodium dodecyl sulfate-polyacrylamide gel electrophoresis (SDS-PAGE) was performed on cell lysates (80 μg per lane). The results are representative of three independent experiments.

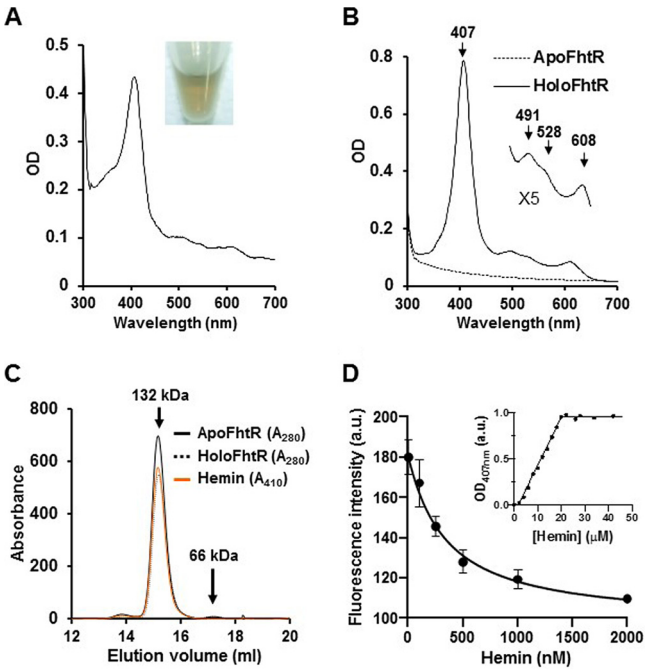

FIG 3 FhtR binds heme. (A) UV-visible absorption spectra of MBP-FhtR as purified from *E. coli*. UV-visible spectra of 30 μM (in 200 μl) MBP-FhtR was obtained in a microplate spectrophotometer (Spark; Tecan) and normalized to an OD_{280} of 1. (Inset) Photograph of the purified MBP-FhtR. Results are representative of three independent experiments. (B) UV-visible spectra of apoMBP-FhtR complexed with hemin. MBP-FhtR was purified from *E. coli* (*hemA*::*kan*) strain as an apoprotein (dashed line) that was mixed with equimolar concentration of hemin. Spectra was obtained as described above for panel A with 20 μM complex and normalized to an OD_{280} of 1. (Inset) Magnification of the 500- to 700-nm region. Results are representative of three independent experiments. (C) Size-exclusion chromatography of apo- and holo-MBP-FhtR. MBP-FhtR was purified and complexed with hemin as described above for panel B. 40 μM of the complex in 100 μl was loaded on a Superdex 200 Increase 10/300 GL gel filtration column (GE Healthcare) in 20 mM HEPES (pH 7), 300 mM NaCl buffer. Protein and heme content were analyzed at OD_{280} and OD_{410}. The results are representative of three independent experiments. (D) Titration of MBP-FhtR with hemin followed by fluorescence and absorbance (inset). For the fluorescence experiment, 50 nM ApoMBP-FhtR purified from *E. coli* (*hemA*::*kan*) as described for panel B were titrated with increasing increments of hemin. Fluorescence intensity (in arbitrary units [a.u.]) was recorded and plotted against hemin concentration. The experiment was repeated three times, fitted using the nonlinear regression function of GraphPad Prism 4 software, and gave a K_d of 310 nM. The inset depicts the absorbance at 407 nm of ApoMBP-FhtR plotted against hemin concentration. The curve is representative of 10 independent experiments and was fitted using the nonlinear regression function of GraphPad Prism 4 software, which determined that the stoichiometry of the FhtR-hemin complex was 1:1.

to the size of a dimer (132 kDa), in line with other TetR regulators (Fig. 3C) (25). The 608-nm charge transfer band and Soret at 407 nm are indicative of a ferric high-spin tyrosinate-ligated heme where heme is anchored through a proximal tyrosinate side chain (27, 28). Hemin pentacoordinate high-spin ligation to FhtR was further confirmed by electron paramagnetic resonance (EPR) spectroscopy (see below). The heme dissociation coefficient (K_d) was 310 nM as determined by MBP-FhtR fluorescence quenching over increasing concentrations of hemin (Fig. 3D). Heme titration by differential absorption spectroscopy at 407 nm showed that the saturation point corresponded to the binding of one molecule of hemin per MBP-FhtR monomer (Fig. 3D, inset). Altogether, these data demonstrate that FhtR is a heme binding protein, suggesting that heme interaction is the primary event leading to activation of $hrtBA_{Ef}$ transcription.

Tyrosine 132 is a crucial heme axial ligand in FhtR. According to UV-visible and EPR spectra, the likely candidate for axial ligand of oxidized heme is a tyrosine (Y) (see above). Several Y residues present in FhtR were substituted to phenylalanine (F) (Fig. S3A, in blue). F and Y both have phenyl ring structures, so that F substitution minimizes an impact on FhtR conformation. Although F lacks the hydroxyl group that

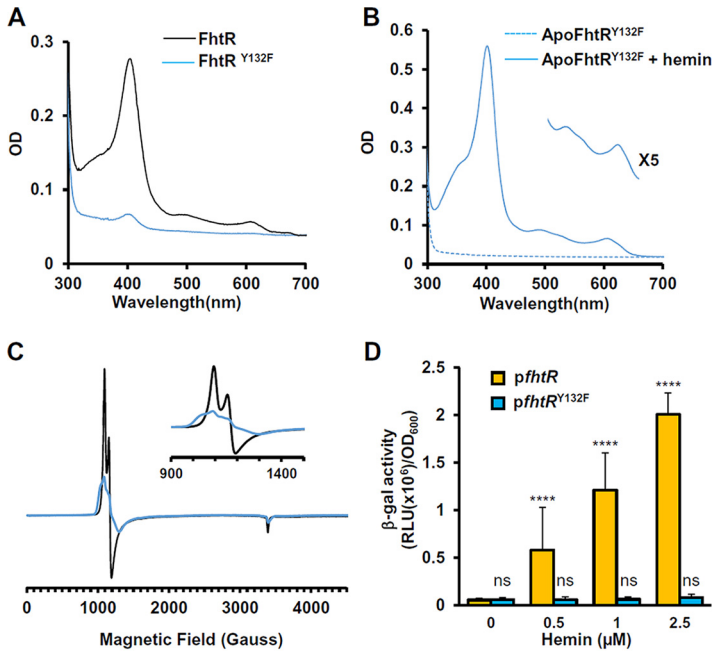

FIG 4 Ligation of FhtR with hemin implicates the tyrosine Y132. (A) Comparative UV-visible absorption spectra of 20 μM MBP-FhtR and MBP-FhtR^{Y132F} purified from *E. coli*. UV-visible spectra were performed as described in the legend to Fig. 3A. The results are representative of three independent experiments. (B) UV-visible spectra of apoMBP-FhtR^{Y132F} complexed with hemin. MBP-FhtR^{Y132F} was purified from *E. coli* (*hemA*::*kan*) strain as an apoprotein (dashed line) that was mixed with equimolar concentration of hemin (holoMBP-FhtR). Spectra were obtained as described for panel A with 20 μM complex and normalized to an OD_{280} of 1. (Inset) Magnification of the 500- to 700-nm region. Results are representative of three independent experiments. (C) EPR spectroscopy of MBP-FhtR and MBP-FhtR^{Y132F} in complex with hemin. EPR spectra of 60 μM bound hemin to WT (black line) and Y132 mutant (blue line) MBP-FhtR in 20 mM HEPES (pH 7) and 300 mM NaCl were recorded. (Inset) Magnification of the 900- to 1,500-gauss magnetic field range. The results are representative of three independent experiments. (D) Induction of the $hrtBA_{Ef}$ operon by hemin. β-gal activity from the Δ*fhtR* strain transformed either with pP$_{hrtBA}$-*lac*, P$_{fhtR}$-*fhtR* or pP$_{hrtBA}$-*lac*, or P$_{fhtR}$-fhtR^{Y132F} was determined as described in the legend to Fig. 1C following incubation with the indicated concentrations of hemin. Results represent the means plus standard deviations from three biological replicates. Statistical significance was determined by one-way analysis of variance (ANOVA) with Dunnett's multiple-comparison test comparing each concentration of hemin to p*fhtR* (0 μM) control with statistical significance indicated as follows: ns, not significant ($P > 0.5$); ****, $P < 0.0001$.

coordinates heme, FhtR heme binding was not modified for several mutants tested individually (Fig. S3A). Only FhtR^{Y132F} was purified from *E. coli* with a strong decrease in heme content compared to WT MBP-FhtR, indicating a loss of heme affinity *in vivo* (Fig. 4A). Surprisingly, apoMBP-FhtR^{Y132F} purified from *hemA*::*kanA E. coli* exhibited similar UV-visible spectra (Fig. 4B) and K_d upon hemin addition (data not shown), questioning the implication of this tyrosine in heme binding. The role of Y132 was further analyzed by EPR spectroscopy (Fig. 4C). HoloMBP-FhtR exhibited an axial high-spin ($S = 5/2$) heme signal with two well-defined resonances at around $g \sim 6$ (with a crossing point at 1,190 G) (Fig. 4C, inset) and a resonance at $g \sim 2$ (~3,390 G), indicative of a 5-coordinated Fe^{III} structure. Although the UV-visible spectra of FhtR and FhtR^{Y132F} supplemented with hemin do not differ to a detectable level, the EPR spectra of FhtR^{Y132F} was significantly modified, thus showing that either the ligand of the iron has been exchanged for another one or more likely, the interaction of the axial ligand with its environment has been modified. To conciliate these results, it is possible that while Y132 is the primary ligand, another distal ligand can take over ligation in the Y132F mutant to become the dominant ligand *in vitro* (meanwhile hydrophobic contacts would ensure retention of the binding affinity).

We then compared FhtR and FhtR^{Y132F} activities *in vivo*. The Δ*fhtR* mutant was complemented either with p*fhtR* (pP$_{hrtBA}$-*lac*; P$_{fhtR}$-*fhtR*) or p*fhtR*^{Y132F} (pP$_{hrtBA}$-*lac*; P$_{fhtR}$-

fhtR^{Y132F}), and β-gal expression was monitored upon hemin addition to medium (Fig. 4D). WT FhtR and FhtR^{Y132F} were expressed to similar levels as confirmed on WB (Fig. S3B). Expression of both proteins prevented *hrtBA*$_{Ef}$ transcription in the absence of heme, in contrast to full expression in Δ*fhtR* (Fig. 4D). WT FhtR and FhtR^{Y132F} were expressed to similar levels as confirmed on WB (Fig. S3B). However, hemin addition led to P$_{hrtBA}$-*lac* expression in the strain carrying WT FhtR, but not FhtR^{Y132F}, suggesting that heme derepression was impaired (Fig. 4D). Altogether, these data specify FhtR Y132 as a critical residue in the coordination of heme with FhtR, which enables *hrtBA*$_{Ef}$ transcription.

FhtR controls *hrtBA*$_{Ef}$ transcription by binding two distinct 14-nt palindromic repeat sequences. TetR family operators usually comprise a 10- to 30-nucleotide (nt) inverted repeat sequence with internal palindromic symmetry (25). Two such 14-nt-long palindromes were identified in the −10/−35 region of the *hrtBA*$_{Ef}$ promoter (called P1 and P2; Fig. 5A). An electrophoretic mobility shift assay (EMSA) was performed with apoMBP-FhtR, using a 325-bp DNA segment comprising the *hrtBA*$_{Ef}$ promoter (Fig. 5B) or a segment covering the internal *hrtB* region as a control (Fig. S4). FhtR-specific interaction with the P$_{hrtBA}$ DNA segment confirmed FhtR binding specificity. The shifted DNA migrated as two distinct bands (C1 and C2), in proportions that depended on the MBP-FhtR: DNA ratio (Fig. 5B), plausibly revealing that FhtR complexes with either one or two palindromes (Fig. 5B). To test this, we performed random substitutions of P1 and/or P2 nucleotides (P1* and P2*) and analyzed DNA shifts by EMSA. Replacement of both distal and proximal operators (P$_{hrtBA\ P1*,\ P2*}$) abolished the FhtR-induced DNA shift, confirming the role of palindromes in the interaction of FhtR with P$_{hrtBA}$ (Fig. 5C). Single replacement of P1 (P$_{hrtBA\ P1*}$) or P2 (P$_{hrtBA\ P2*}$) resulted in complete DNA shifts that migrated faster in the gel (C1) than seen with the native nucleotide sequence (Fig. 5C). We conclude that both P1 and P2 are FhtR binding sites.

We then tested the effects of heme on FhtR binding by EMSA. Addition of hemin to MBP-FhtR abolished the formation of the DNA-FhtR complex, as seen by the progressive disappearance of band shifts with increasing hemin concentrations (Fig. 5D). Complete release of FhtR from P$_{hrtBA}$ was obtained when hemin was in 10-fold molar excess over FhtR (Fig. 5D). Both C1 and C2 complexes were revealed when intermediate amounts of heme were added (0.1 and 1 μM; Fig. 5D). This suggests the release of MBP-FhtR from only one operator depending on the saturation level of FhtR with hemin.

The role of the two operators in the control of *hrtBA*$_{Ef}$ was investigated *in vivo*, using P$_{hrtBA}$ or a P$_{hrtBA\ P1*,\ P2*}$ promoter variant to control *lac* gene (Fig. 5E). In contrast to pP$_{hrtBA}$-*lac*, which was strongly induced with 1 μM hemin, P$_{hrtBA\ P1*,\ P2*}$-*lac* was constitutively expressed (Fig. 5E). Finally, the role of each operator was investigated (Fig. 5F). In the absence of heme, either P1 or P2 is sufficient for full P$_{hrtBA}$ repression by FhtR. Release of the promoter was facilitated in the presence of only P1 or P2 as shown with increased transcriptional activities of P$_{hrtBA\ P1*}$ or P$_{hrtBA\ P2*}$ in the presence of hemin compared to native P$_{hrtBA}$ (Fig. 5F). We propose that the presence of two operators provides strong repression of the *hrtBA*$_{Ef}$ promoter, thus preventing transcriptional leakage and allowing for fine tuning of HrtBA$_{Ef}$ expression. Taken together, these results demonstrate that FhtR is a heme sensor that directly controls heme homeostasis by regulating *hrtBA*$_{Ef}$ transcription.

FhtR controls HrtBA$_{Ef}$, the gatekeeper of intracellular heme availability. Our observation that FhtR regulates intracellular heme pools even at low heme concentrations led us to hypothesize that FhtR controls intracellular heme availability in *E. faecalis*. We tested this possible role of FhtR on the *E. faecalis* endogenous heme-dependent catalase (KatA). While *katA* transcription is not susceptible to heme induction, KatA protein stability relies on the presence of heme (10, 12). KatA-mediated H_2O_2 catalysis was measured in WT, Δ*fhtR*, and Δ*fhtR*(p*fhtR*) strains (Fig. 6A). In the absence of hemin, H_2O_2 consumption was at a basal level (Fig. S5A), thus excluding major contributions of other enzymes in our conditions. In the presence of 1 μM hemin (Fig. 6A), the Δ*fhtR* mutant exhibited about 30% catalase activity compared to WT and complemented

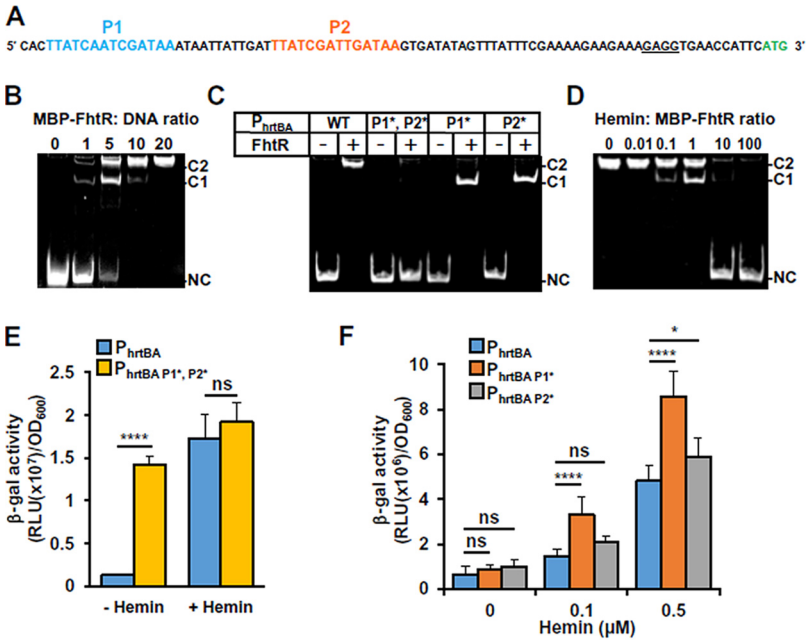

FIG 5 FhtR controls $hrtBA_{Ef}$ transcription via binding to two repeated 14-nt palindromic sequences. (A) Two 14-nt palindromic motifs are present upstream of $hrtBA_{Ef}$. The two palindromes are shown in blue (P1) and in red (P2); the ribosome binding sequence (RBS) is underlined, and the start codon is shown in green. (B) FhtR binds to the promoter region of $hrtBA_{Ef}$. EMSA shows binding of FhtR to P_{hrtBA}. The $hrtBA_{Ef}$ promoter fragment (0.25 pmol) was incubated with increasing amounts of MBP-FhtR as indicated in molar ratios. DNA shift was visualized with GelRed (Biotium) following PAGE. The two shifted DNA-protein complexes (C1 and C2) and noncomplexed DNA (NC) are indicated. The results are representative of at least three independent experiments. (C) Roles of P1 and P2 on FhtR binding to the promoter region of $hrtBA_{Ef}$. EMSA was performed as described for panel B with either the native P_{hrtBA} DNA fragment (WT) (as in panel A) or mutated fragments $P_{hrtBA\ P1^*,\ P2^*}$, $P_{hrtBA\ P1^*}$, and $P_{hrtBA\ P2^*}$. MBP-FhtR: DNA (2.5 pmol: 0.25 pmol). The results are representative of at least three independent experiments. (D) Effect of hemin on the binding of FhtR to the $hrtBA_{Ef}$ promoter. The $hrtBA_{Ef}$ promoter DNA (0.25 pmol) was incubated with 2.5 pmol of MBP-FhtR together with increasing amounts of hemin as indicated (molar ratios) and analyzed by EMSA as described in the legend to panel B. The results are representative of at least three independent experiments. (E) Substitution of the two palindromic nucleotide sequences, P1 and P2, in P_{hrtBA} abrogates FhtR-mediated control of $hrtBA_{Ef}$ transcription. The WT strain was transformed either with the reporter plasmid pP_{hrtBA}-*lac* or $pP_{hrtBA\ P1^*P2^*}$ -*lac*. β-Gal activity was determined as described in the legend to Fig. 1 following incubation with 2.5 μM hemin. Results represent the means plus standard deviations from three biological replicates. Statistical significance was determined by *t* test with statistical significance indicated as follows: ns, not significant ($P > 0.5$); ****, $P < 0.0001$. (F) Substitution of either P1 or P2 nucleotide sequences in P_{hrtBA} enhances its transcriptional activation by hemin. The WT strain was transformed either with the reporter plasmid pP_{hrtBA}-*lac*, $pP_{hrtBA\ P1^*}$ -*lac*, or $pP_{hrtBA\ P2^*}$ -*lac*. β-Gal activity was determined as described in the legend to Fig. 1 following incubation with hemin. Results represent the means plus standard deviations from three biological replicates. Statistical significance was determined by one-way ANOVA with Tukey's multiple-comparison test with significance indicated as follows: ns, not significant ($P > 0.5$); *, $P = 0.0140$; ****, $P < 0.0001$.

Δ*fhtR*(p*fhtR*) strains, as evaluated by the percentage of catabolized H_2O_2 (Fig. 6A). This was further confirmed by comparing the amounts of KatA (holoKatA) by WB, using anti-KatA antibody (kindly provided by L. Hederstedt). In the absence of hemin, KatA was expressed at low levels in WT, Δ*fhtR*, and Δ*fhtR*(p*fhtR*) strains (Fig. 6B). Comparatively, addition of hemin strongly increased the amounts of KatA in WT and complemented Δ*fhtR*(p*fhtR*) strains, but not in the Δ*fhtR* mutant (Fig. 6B). Low KatA availability in the Δ*fhtR* mutant is readily explained by constitutive heme efflux (via $HrtBA_{Ef}$), and consequently depleted intracellular heme pools in this mutant. We then evaluated the survival capacity of *E. faecalis* OG1RF WT, Δ*fhtR*, and Δ*fhtR*(p*fhtR*) strains when challenged with 2.5 mM H_2O_2. In the absence of hemin, all strains grew equivalently without H_2O_2 (Fig. S5B). In contrast, while hemin addition rescued the survival of both the WT and Δ*fhtR*(p*fhtR*) strains, the Δ*fhtR* strain remained hypersensitive to H_2O_2

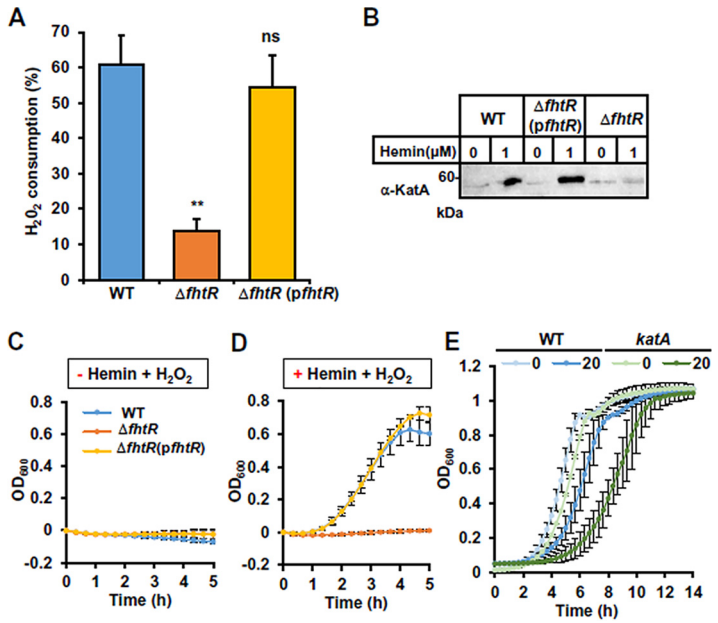

FIG 6 FhtR controls intracellular utilization of heme. (A) *fhtR* deletion limits heme-dependent KatA activity. KatA enzymatic activity in *E. faecalis* was assessed on WT, Δ*fhtR*, and Δ*fhtR*(p*fhtR*) grown overnight (ON) with 1 μM hemin. Catalase activity was determined on an equivalent number of bacteria incubated with 100 μM H_2O_2 for 1 h with the spectrophotometric FOX1 method based on ferrous oxidation in xylenol orange. Results are expressed as the percentage of H_2O_2 metabolized in respective strains grown without hemin. Results represent the means plus standard deviations from three biological replicates. Statistical significance was determined by one-way analysis of variance (ANOVA) with Dunnett's multiple-comparison test comparing each strain to the WT strain control with significance indicated as follows: ns, $P > 0.05$; **, $P = 0.008$. (B) Expression of KatA is impaired in the Δ*fhtR* mutant. Equivalent amounts of protein (20 μg) from lysates of WT, Δ*fhtR*, and Δ*fhtR*(p*fhtR*) strains as described for panel A were separated by SDS-PAGE, and immunoblots were probed with an anti-KatA polyclonal antibody. The presented results are representative of three independent experiments. (C and D) The Δ*fhtR* mutant is hypersensitive to H_2O_2. ON cultures of WT, Δ*fhtR*, and Δ*fhtR*(p*fhtR*) strains were diluted to an OD_{600} of 0.01 and grown to an OD_{600} of 0.5 in the absence of hemin (C) or in the presence of 1 μM hemin (D). Cultures were distributed in wells on a 96-well plate and supplemented with 2.5 mM H_2O_2 or not supplemented with H_2O_2. OD_{600} was monitored every 20 min in a microplate spectrophotometer (Spark; Tecan). OD_{600} at time zero was normalized to 0. Results represent the means ± standard deviations from three biological replicates. (E) KatA limits heme toxicity. ON cultures of WT and *katA*::*tetR* strains were diluted to an OD_{600} of 0.01 and grown in 96-well plate in the presence of the indicated concentration of hemin as described for panel D. Results represent the means ± standard deviations from three biological replicates.

(Fig. 6C and D). Deletion of $hrtBA_{Ef}$ in the Δ*fhtR* strain (Δ*fhtR* Δ$hrtBA_{Ef}$) restored the survival capacity in the presence of hemin (Fig. S5C). Thus, poor survival of Δ*fhtR* reflects the lack of heme needed to stabilize KatA (Fig. 6D). Finally, the OG1RF mutant (*katA*::*tetR*) was hypersensitive to hemin toxicity, showing that KatA was required for controlling oxidative stress generated by heme (Fig. 1E and Fig. 4E). Taken together, these results identify FhtR as the direct and indirect regulator of $HrtBA_{Ef}$-mediated heme efflux and KatA activity, respectively, with both mechanisms lowering heme stress in *E. faecalis* OG1RF. FhtR is thus a key mediator of heme homeostasis, and consequently, of oxidative stress response in *E. faecalis* generated by H_2O_2.

Heme sensing in the gastrointestinal tract. *E. faecalis* is a normal resident of the GIT of vertebrates, an ecosystem where heme is available (29–32). We therefore investigated whether $hrtBA_{Ef}$-mediated heme management is required by *E. faecalis* in the GIT in a murine gastrointestinal model. We generated *E. faecalis* OG1RF strains expressing the *luxABCDE* (*lux*) operon from *Photorhabdus luminescens* driven by the following: (i) P_{hrtBA} (pP_{hrtBA}-*lux*), which emits light specifically in the presence of hemin (Fig. 7A); (ii) a constitutive promoter P23 (p*lux*), constitutively emitting light for bacterial tracking (14); or (iii) a control promoterless vector, $pP_{\varnothing}$-*lux*. Cultures of these strains were

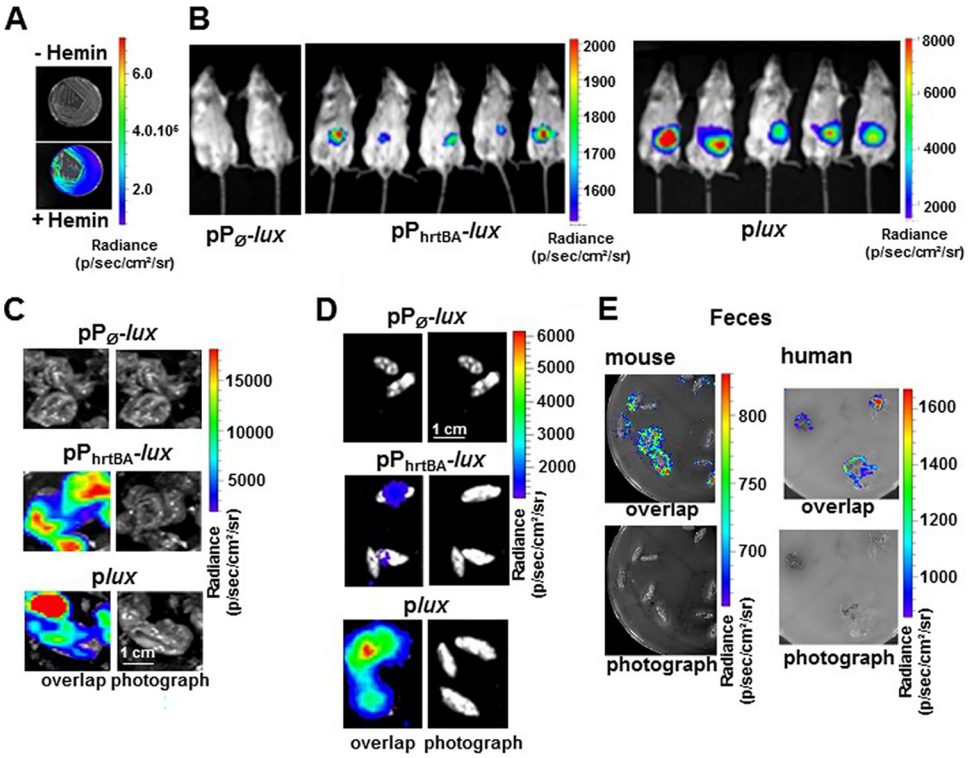

FIG 7 HrtBA$_{Ef}$ is induced in the gastrointestinal environment. (A) Heme-dependent light emission by the heme sensing WT(pP$_{hrtBA}$-*lux*) strain. WT(pP$_{hrtBA}$-*lux*) was plated on M17G agar plates in the presence (+) or absence (−) of 20 μM hemin. Plates were incubated at 37°C for 24 h, and luminescence was visualized using an IVIS 200 luminescence imaging system (acquisition time, 1 min; binning 8). Radiance is shown in photons per second per square centimeter per steradian. The results are representative of three independent experiments. (B) Heme sensing by *E. faecalis* over the course of intestinal transit. Female BALB/c mice were force fed with 10^8 CFU of WT(pP$_{ø}$-*lux*) (control strain), WT(pP$_{hrtBA}$-*lux*) (sensor strain), or WT(p*lux*) (tracking strain). At 6 h postinoculation, anesthetized mice were imaged in the IVIS 200 system (acquisition time, 20 min; binning 16). The figure shows representative animals corresponding to a total of 15 animals for each condition in three independent experiments. (C) Ceca exhibit high heme sensing signal. Animals as described above for panel B were euthanized and immediately dissected. Isolated GITs were imaged as described above for panel B. Ceca that exhibited most of the luminescence are shown (acquisition time, 5 min; binning 8). Bar = 1 cm. (D) Visualization of heme sensing in feces collected from mice following ingestion of WT(pP$_{ø}$-*lux*), WT(pP$_{hrtBA}$-*lux*), or WT(p*lux*). WT(pP$_{hrtBA}$-*lux*) as described above for panel B were collected 6 to 9 h after gavage. Feces were imaged as described above for panel B (acquisition time, 20 min; binning 16). Bar = 1 cm. Results are representative of three independent experiments. (E) Human and mouse fecal samples activate heme sensing. Human feces from three healthy human laboratory volunteers and mouse feces from 6-month-old female BALB/c mice were deposited on M17G agar plates layered with soft agar containing WT OG1RF (pP$_{hrtBA}$-*lux*). Plates were incubated at 37°C for 16 h and imaged in the IVIS 200 system (acquisition time, 10 min; binning 8). The figure shows representative results of a total of three independent experiments.

orally inoculated in the digestive tracts of mice, and light emission from whole live animals was measured in an *in vivo* imaging system IVIS200, 6 h postinoculation (Fig. 7B). This time delay corresponded to the maximum light emission from the tracking strain OG1RF(p*lux*) (Fig. S6A). Luminescence signaling from the ingested *E. faecalis* pP$_{hrtBA}$-*lux* heme sensor strain also localized in the abdomen, similar to the tracking strain (Fig. 7B). Examination of dissected organs revealed that the heme sensor-associated luminescence was mainly detected in the cecum (Fig. 7C), correlating with the high bacterial load of this organ [WT(p*lux*); Fig. 7C]. A significant signal was also detected in the feces from inoculated animals, further highlighting that *E. faecalis* was able to scavenge and internalize heme within the digestive tract to induce *hrtBA*$_{Ef}$ expression (Fig. 7D). Finally, mice and human fecal samples (as well as fecal waters [Fig. S6B and S6C]) from healthy individuals were able to induce luminescence from WT(pP$_{hrtBA}$-*lux*) *in vitro*, excluding the possibility that induction of P$_{hrtBA}$ *in vivo* could result from the inoculation procedure (Fig. 7E). Therefore,

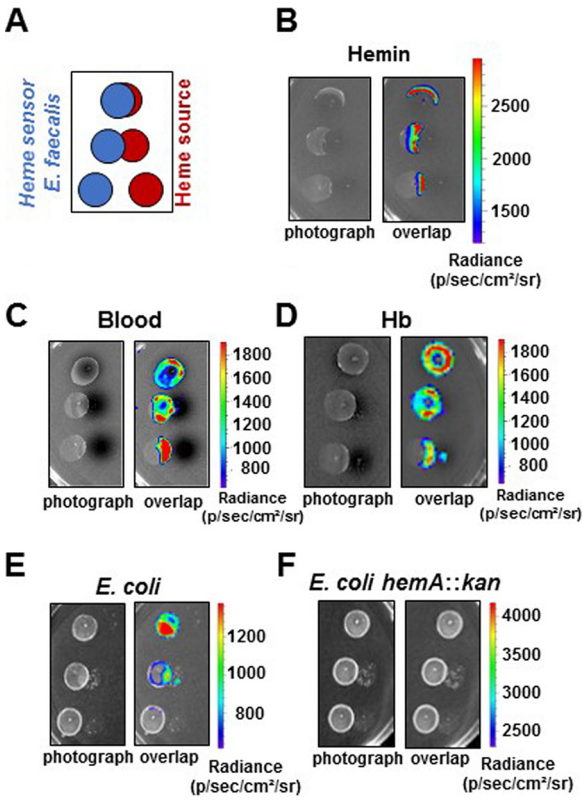

FIG 8 Heme sources for *E. faecalis* in the GIT. (A) Intracellular heme sensing setup. The indicated heme sources (10 μl) are deposited on M17G solid medium as shown in red. The WT (pP_{hrtBA}-*lux*) heme sensor plasmid is plated as 10-μl spots at an OD_{600} of 0.01 as shown in blue. The plates were incubated at 37°C for 16 h and imaged in the IVIS 200 system (acquisition time, 10 min; binning 8). The results are representative of three independent experiments. (B) Visualization of heme sensing from hemin deposits. Hemin (1 mM) in PBS was used as described above for panel A. (C and E) Heme from blood (bovine) and hemoglobin (human) are heme sources for *E. faecalis*. Heparinized bovine blood (Thermo Fisher) and freshly dissolved human hemoglobin (1 mM) in PBS were used as described above for panel A. (F and G) *E. coli* is a heme donor for *E. faecalis*. *E. coli* (NEB10; New England Biolabs) (F) or a mutant strain that cannot synthesize heme (*hemA*::*kan*) (G) at an OD_{600} of 0.1 were deposited on M17G plates as described above for panel A. Only the heme-synthesizing strain was able to crossfeed heme to *E. faecalis*. Panels B to F show representative results of three independent experiments.

FhtR heme sensor activity is active and relevant to *E. faecalis* heme management in the lumen of the GIT.

Heme sources for *E. faecalis* in the GIT. The results described above imply that *E. faecalis* internalizes heme in the intestinal environment to activate FhtR. Thus, an interesting question remains as to the identities of heme sources that are accessible to *E. faecalis* in the GIT. Normal bleeding (occult blood), exacerbated in intestinal pathologies, as well as food (as meat) are considered main sources of heme within the GIT (the second being excluded in mice) (29–32). We thus visualized the ability of hemoglobin (Hb) or blood deposited on plates as schematized (Fig. 8A) to induce P_{hrtBA} from the heme sensor strain WT(pP_{hrtBA}-*lux*) as shown with hemin (Fig. 8B). Similarly, luminescence was induced in proximity of Hb and blood deposits as heme sources (Fig. 8C and D). This result suggests that heme from physiologically available sources is internalized by *E. faecalis*. Crossfeeding of metabolites, including heme between bacteria, has been reported (29, 33). The possibility that *E. faecalis* could scavenge heme from intestinal resident heme-synthesizing bacteria, such as *E. coli*—a phylum that becomes prevalent together with *E. faecalis* throughout dysbiosis—was evaluated. The WT (pP_{hrtBA}-*lux*) heme sensor strain was grown in contact with *E. coli* (as the heme source) as illustrated in Fig. 8A. Strikingly, induction of luminescence was localized to areas of

overlap between the two bacteria (Fig. 8E) and required heme synthesis by *E. coli*, as no sensing could be detected with a heme-defective *hemA*::*kan* mutant (Fig. 8F). This result suggests that heme synthesized by *E. coli* is internalized by *E. faecalis*. Thus, heme crossfeeding between bacterial symbionts in the gut might provide a heme source for *E. faecalis*. We conclude that the *E. faecalis* heme sensor is activated by the heme sources available in the GIT.

DISCUSSION

E. faecalis is a core member of the microbiome, and it is also the cause of a variety of severe infections (34). The central role of heme in reprogramming *E. faecalis* metabolism and fitness led us to investigate how heme homeostasis is controlled. A novel heme sensor, FhtR, is shown here to regulate heme intracellular homeostasis in *E. faecalis*. FhtR-heme complexes derepress the $hrtBA_{Ef}$ operon, leading to HrtBA-mediated management of intracellular heme pools. While expression of HrtBA is a conserved strategy in multiple Gram-positive organisms, *E. faecalis* appears to be the first example of an opportunistic pathogen where HrtBA is not controlled by the two-component system HssRS. BLAST analysis of FhtR homologs in several Gram-positive bacteria showed that the regulator is present only in enterococci, vagococci, and carnobacteria (see Fig. S7A and S7B in the supplemental material for FhtR alignments and phylogenic tree). FhtR shares no homology with HrtR, a TetR regulator of *hrtRBA* in *Lactococcus lactis* (19). In contrast to HrtR which autoregulates its own expression, *fhtR* is monocistronic and expressed constitutively, implying that only $HrtBA_{Ef}$ expression is controlled by heme (19).

We characterized FhtR as a heme binding protein through pentacoordinated ligation of the heme iron, implying a tyrosine. This state of coordination is mostly found in heme receptors that transiently bind heme, such as IsdA, IsdC, and IsdH in *S. aureus* or HmA in *Escherichia coli* (35). FhtR blocks $hrtBA_{Ef}$ transcription by binding to two distinct 14-nt inverted repeats sequences in its promoter region. Alleviation of repression occurs when the heme-FhtR complex loses its affinity for its DNA binding sites. Conformational changes upon ligand binding is a shared mechanism among TetR regulators, leading to uncoupling from DNA (26). We thus hypothesize that these events, which we verified *in vitro*, explain FhtR regulation of the $hrtBA_{Ef}$ efflux pump in *E. faecalis*. The unique features of FhtR in *E. faecalis* compared to other regulators of *hrtBA* genes encoding efflux pumps support the idea that control of HrtBA-mediated heme homeostasis may vary among bacteria as a function of their lifestyle. It is thus tempting to speculate that differences in host niches, and in heme utilization and metabolism, might explain disparities in bacterial heme sensing mechanisms.

Heme efflux by HrtBA is reported as a bacterial detoxification mechanism that prevents intracellular heme overload (8, 14, 16, 17, 19). We showed here that HrtBA induction is required for *E. faecalis* survival when heme concentrations reached toxic levels ($>25\,\mu$M). Yet, $hrtBA_{Ef}$ was induced at heme concentrations as low as $0.1\,\mu$M, suggesting that heme efflux is also needed at nontoxic levels. Interestingly, *E. faecalis* carries a gene that encodes the heme-dependent catalase whose activity relies on the amount of heme in the cytoplasm that is indirectly regulated by FhtR. This enzyme not only binds heme and thus lowers free heme levels, but it also actively lowers oxidative stress generated by heme. It will be of interest to determine the hierarchy of heme binding between FhtR and catalase *in vivo*.

To date, no heme import function has been identified in *E. faecalis* or in other tested Gram-positive bacteria that cannot synthesize heme (13, 18). BLAST analysis of these bacteria failed to identify genes of the *isd* heme import system described in *Staphylococcus aureus* (36, 37). In *S. aureus*, heme receptors and transporters are induced in iron-depleted growth media, and imported heme is used as an iron source (36). Thus, our findings led us to question the need for a dedicated transport system to internalize exogenous heme in *E. faecalis* and to propose an alternative hypothesis. We noted that $HrtBA_{Ef}$ is a member of the MacB family of efflux pumps that is distinct from other structurally characterized ABC transporters (38). A model based on MacB

transport of antibiotics and antimicrobial peptides in *Streptococcus pneumoniae* proposed that transmembrane conformational changes promote lateral entry of substrates in the membrane before they reach the cytoplasm (39). On the basis of the previous and present data (23), we propose that $HrtB_{Ef}$ has the integral role as the heme "gatekeeper" in the cell. Like MacB antibiotics and antimicrobial substrates (40), membrane-bound heme could either enter passively into the intracellular compartment and or be effluxed by HrtB before this step. Altogether, our results place $HrtBA_{Ef}$ at the forefront of heme homeostasis in *E. faecalis* that is dependent on the key role of FhtR to adapt to the dichotomy between toxicity and benefits of heme which may be crucial in the host.

In vivo bioluminescence imaging of *E. faecalis* using an FhtR-based sensor identified the GIT as an environment where $HrtBA_{Ef}$ is expressed. The gut lumen of healthy individuals contains heme, independently of the nature of ingested food or of the microbiota (29–32). Heme in the GIT is reported to mainly originate from Hb from normal bleeding (occult blood) (41). Accordingly, *E. faecalis* was able to internalize heme from blood and Hb *in vitro*. In addition, a common microbiota constituent, *Escherichia coli*, is shown to be a heme donor, suggesting a novel basis for intestinal bacterial interactions. As several phyla composing the core microbiota are heme auxotrophs with vital heme requirements, it is tempting to hypothesize that normal or disease-associated fluctuations in host heme levels could be detected by FhtR to adjust its intracellular level and optimize bacterial fitness. Interestingly, *E. faecalis* causes a variety of severe infections, most often among antibiotic-treated hospitalized patients with intestinal dysbiosis favoring high *E. coli* and enterobacterial populations (42). It will be interesting to evaluate the impact of HrtBA and FhtR in *E. faecalis* fitness and virulence in *in vivo* models. Taken together, our results suggest that the FhtR sensor and the $HrtBA_{Ef}$ heme gatekeeper allow *E. faecalis* to optimize its adaptation to variable heme pools in the host.

MATERIALS AND METHODS

Bacterial strains and growth conditions. Bacterial strains and plasmids used in this work are listed in Table S1 in the supplemental material. *E. coli* NEB10 (New England Biolabs) was grown in LB medium, and *E. coli* C600 *hemA*::*kan* was grown in M17 medium supplemented with 0.5% glucose (M17G). Experiments with *E. faecalis* were all performed using strain OG1RF and derivatives (Table S1). *E. faecalis* was grown in static conditions at 37°C in M17G. When needed, antibiotics were used for *E. coli* at 50 μg · ml^{-1} kanamycin and 100 μg · ml^{-1} ampicillin; for *E. faecalis*, 30 μg · ml^{-1} erythromycin was used. Oligonucleotides used for plasmid constructions are listed in Table S2. Hemin (Fe-PPIX) (Frontier Scientific) was prepared from a stock solution of 10 mM hemin chloride in 50 mM NaOH. In this report, heme refers to iron protoporphyrin IX regardless of the iron redox state, whereas hemin refers to ferric iron protoporphyrin IX. For growth homogeneity, WT and mutant strains were transformed with the promoterless pTCV-*lac* plasmid compared to complemented strains. Plasmid construction and *E. faecalis* gene deletion are described in Text S1 in the supplemental material.

β-Galactosidase assays. Stationary-phase cultures were diluted at an optical density at 600 nm (OD_{600}) of 0.01 in M17G and grown to an OD_{600} of 0.5. Hemin was added to cultures, which were further grown for 1.5 h. β-Galactosidase activity was quantified by luminescence in a Spark microplate luminometer (TECAN) using the β-glo substrate (Promega) as described previously (19).

Cellular ROS quantification. Stationary-phase cultures were diluted at an OD_{600} of 0.01 in M17G and grown to an OD_{600} of 0.5. Hemin was added to cultures, which were further grown for 1.5 h. Bacteria were washed twice with phosphate-buffered saline (PBS) plus 0.5% glucose by centrifugation at 4°C to remove extracellular heme. Cell pellets were resuspended in PBS plus 0.5% glucose supplemented with 25 μM dihydrorhodamine 123, a cell-permeant fluorescent ROS indicator (Invitrogen). Cell suspensions were distributed into the wells of a 96-well plate. After 15-min incubation, optical density at 600 nm and fluorescence (excitation 500 nm; emission, 536 nm) were measured in a Spark microplate spectrofluorimeter (Tecan).

Bacterial lysate preparation. Bacteria were pelleted at 3,500 × *g* for 10 min, resuspended in 20 mM HEPES (pH 7.5) and 300 mM NaCl and disrupted with glass beads (Fastprep; MP Biomedicals). Cell debris was removed by centrifugation at 18,000 × *g* at 4°C for 15 min from the bacterial lysate supernatant. Proteins were quantified by the Lowry method (Bio-Rad).

Heme concentration determination in bacterial lysates. Equivalent amounts of proteins (in a volume of 250 μl) were mixed with 250 μl of 0.2 M NaOH, 40% (vol/vol) pyridine, and 500 μM potassium ferricyanide or 5 μl of 0.5 M sodium dithionite (diluted in 0.5 M NaOH), and 500- to 600-nm absorption spectra were recorded in a UV-visible spectrophotometer Libra S22 (Biochrom). Dithionite-reduced minus ferricyanide-oxidized spectra of pyridine hemochromes were used to determine the amount of heme *b* by monitoring the value of the difference between absorbance at 557 nm and 540 nm using a difference extinction coefficient of 23.98 $mM^{-1} \cdot cm^{-1}$ (43).

Recombinant MBP-FhtR purification. MBP-FhtR and MBP-$FhtR^{Y132F}$ were purified by affinity chromatography on amylose resin as reported previously (19). Briefly, *E. coli* NEB10 or C600 Δ*hemA* strains

were grown to an OD_{600} of 0.6 or 0.3, respectively, and expression was induced with 1 mM isopropyl-1-thio-β-D-galactopyranoside (IPTG) overnight (ON) at room temperature (RT). Cells were pelleted at 3,500 $\times$ *g* for 10 min, resuspended in 20 mM HEPES (pH 7.5) and 300 mM NaCl containing 1 mM EDTA (binding buffer), and disrupted with glass beads (Fastprep; MP Biomedicals). Cell debris was removed by centrifugation at 18,000 $\times$ *g* for 15 min at 4°C. MBP-tagged proteins were purified by amylose affinity chromatography (New England Biolabs) following the manufacturer's recommendations: the soluble fraction was mixed with amylose resin and incubated on a spinning wheel at 4°C for 1 h. The resin was then centrifuged and washed three times with binding buffer. Purified proteins were eluted in binding buffer containing 10 mM maltose and dialyzed against 20 mM HEPES (pH 7.5) and 300 mM NaCl.

Heme-dependent catalase expression and activity. KatA expression was monitored on immunoblots with a polyclonal anti-KatA antibody (10). Catalase activity was determined on whole bacteria incubated with 100 μM H_2O_2 with the spectrophotometric FOX1 method based on ferrous oxidation in xylenol orange as described previously (44, 45). Absorption was measured at 560 nm.

Electrophoretic mobility shift assay. A 325-bp DNA fragment containing the $hrtBA_{Ef}$ promoter (P_{hrtBA}) was amplified by PCR from *E. faecalis* OG1RF genomic DNA with primer pair (O21-O22) (Table S2). In P_{hrtBA}, the two 14-nt palindromic sequences P1 (5′-TTATCAATCGATAA-3′) and P2 (5′-TTATCGAT TGATAA-3′) were randomly altered to P1* (5′-ACTTGTATACATAA-3′) and P2* (5′-ATATCTTGTATAAG-3′) to generate three DNA variants $P_{hrtBA\ P1*}$, $P_{hrtBA\ P2*}$, and $P_{hrtBA\ P1*,\ P2*}$. These fragments were cloned into pUC plasmid (pUC-VS1, pUC-VS2, and pUC-VS3; Table S1) (Proteogenix, France) that were used as templates to PCR amplify the promoter region DNA variants with the primer pairs (O21-O22) (Table S2) that were cloned into pTCV (Table S1). EMSA (electrophoretic mobility shift assay) was performed in 20 mM Tris-HCl (pH 8), 50 mM KCl, 0.2 mM $MgCl_2$, 1 mM EDTA, 0.2 mM dithiothreitol (DTT), and 5% glycerol as reported previously (19). Binding was analyzed by gel electrophoresis on a 7% polyacrylamide gel in Tris-borate-EDTA (TBE) buffer stained with GelRed (Biotium) following electrophoresis.

Ethics statement. Animal experiments were conducted in strict accordance with the recommendations in the guidelines of the Code for Methods and Welfare Considerations in Behavioural Research with Animals of the EEC council (Directive 2010/63/EU). The protocols were approved by the Animal Care and Use Committee at the Research center of Jouy-en-Josas (COMETHEA; protocol number 15–61) and by the Ministry of Education and Research (APAFIS 2277-2015081917023093 v4). All efforts were undertaken to minimize animal suffering. All experimental procedures were performed in biosafety level 2 facilities.

***In vivo* heme sensing assay in the mouse GIT.** For inoculation in the digestive tract, *E. faecalis* strains were prepared as follows. *E. faecalis* OG1RF precultures were diluted and grown in M17G to an OD_{600} of 0.5 that was determined to correspond to 6 $\times$ 10^8 CFU/ml. Bacteria were then centrifuged at 6,000 rpm at 4°C for 15 min, and pellets were resuspended in PBS to a final concentration of 2 $\times$ 10^8 cells/ml. Bacterial stocks were aliquoted and frozen in liquid nitrogen. Aliquots were kept at −80°C until use. Bacterial counts were confirmed by plating serial dilutions of cultures. Six-week-old female BALB/c mice (Janvier, France) were orally administered by gavage of 10^8 CFU using a feeding tube. Image acquisition of isoflurane-anesthesized mice was performed at the indicated time following gavage. Following image acquisition, mice were removed from the IVIS 200 imaging system and immediately sacrificed by cervical dislocation. When indicated, the animals were dissected for imaging of the isolated organs. The *in vivo* luminescence imaging procedure is described in Text S1 in the supplemental material.

SUPPLEMENTAL MATERIAL

Supplemental material is available online only.

TEXT S1, DOCX file, 0.03 MB.

FIG S1, TIF file, 2.4 MB.

FIG S2, TIF file, 2.2 MB.

FIG S3, TIF file, 2.3 MB.

FIG S4, TIF file, 1.7 MB.

FIG S5, TIF file, 2.9 MB.

FIG S6, TIF file, 2.7 MB.

FIG S7, TIF file, 2.8 MB.

TABLE S1, DOCX file, 0.02 MB.

TABLE S2, DOCX file, 0.01 MB.

REFERENCES

1. Arias CA, Murray BE. 2012. The rise of the Enterococcus: beyond vancomycin resistance. Nat Rev Microbiol 10:266–278. https://doi.org/10.1038/nrmicro2761.
2. Agudelo Higuita NI, Huycke MM. 2014. Enterococcal disease, epidemiology, and implications for treatment. *In* Gilmore MS, Clewell DB, Ike Y, Shankar N (ed), Enterococci: from commensals to leading causes of drug resistant infection. Massachusetts Eye and Ear Infirmary, Boston, MA.
3. Mendes RE, Castanheira M, Farrell DJ, Flamm RK, Sader HS, Jones RN. 2016. Longitudinal (2001–14) analysis of enterococci and VRE causing invasive infections in European and US hospitals, including a contemporary (2010-13) analysis of oritavancin in vitro potency. J Antimicrob Chemother 71:3453–3458. https://doi.org/10.1093/jac/dkw319.
4. Van Tyne D, Gilmore MS. 2017. Raising the alarmone: within-host evolution of antibiotic-tolerant *Enterococcus faecium*. mBio 8:e00066-17. https://doi.org/10.1128/mBio.00066-17.
5. Gruss A, Borezee-Durant E, Lechardeur D. 2012. Environmental heme

utilization by heme-auxotrophic bacteria. Adv Microb Physiol 61:69–124. https://doi.org/10.1016/B978-0-12-394423-8.00003-2.
6. Pishchany G, Skaar EP. 2012. Taste for blood: hemoglobin as a nutrient source for pathogens. PLoS Pathog 8:e1002535. https://doi.org/10.1371/journal.ppat.1002535.
7. Kumar S, Bandyopadhyay U. 2005. Free heme toxicity and its detoxification systems in human. Toxicol Lett 157:175–188. https://doi.org/10.1016/j.toxlet.2005.03.004.
8. Anzaldi LL, Skaar EP. 2010. Overcoming the heme paradox: heme toxicity and tolerance in bacterial pathogens. Infect Immun 78:4977–4989. https://doi.org/10.1128/IAI.00613-10.
9. Wakeman CA, Hammer ND, Stauff DL, Attia AS, Anzaldi LL, Dikalov SI, Calcutt MW, Skaar EP. 2012. Menaquinone biosynthesis potentiates haem toxicity in *Staphylococcus aureus*. Mol Microbiol 86:1376–1392. https://doi.org/10.1111/mmi.12063.
10. Frankenberg L, Brugna M, Hederstedt L. 2002. *Enterococcus faecalis* heme-dependent catalase. J Bacteriol 184:6351–6356. https://doi.org/10.1128/JB.184.22.6351-6356.2002.
11. Winstedt L, Frankenberg L, Hederstedt L, Von Wachenfeldt C. 2000. *Enterococcus faecalis* V583 contains a cytochrome bd-type respiratory oxidase. J Bacteriol 182:3863–3866. https://doi.org/10.1128/jb.182.13.3863-3866.2000.
12. Brugna M, Tasse L, Hederstedt L. 2010. In vivo production of catalase containing haem analogues. FEBS J 277:2663–2672. https://doi.org/10.1111/j.1742-464X.2010.07677.x.
13. Hammer ND, Reniere ML, Cassat JE, Zhang Y, Hirsch AO, Indriati Hood M, Skaar EP. 2013. Two heme-dependent terminal oxidases power *Staphylococcus aureus* organ-specific colonization of the vertebrate host. mBio 4:e00241-13. https://doi.org/10.1128/mBio.00241-13.
14. Joubert L, Dagieu JB, Fernandez A, Derre-Bobillot A, Borezee-Durant E, Fleurot I, Gruss A, Lechardeur D. 2017. Visualization of the role of host heme on the virulence of the heme auxotroph *Streptococcus agalactiae*. Sci Rep 7:40435. https://doi.org/10.1038/srep40435.
15. Baureder M, Hederstedt L. 2013. Heme proteins in lactic acid bacteria. Adv Microb Physiol 62:1–43. https://doi.org/10.1016/B978-0-12-410515-7.00001-9.
16. Fernandez A, Lechardeur D, Derre-Bobillot A, Couve E, Gaudu P, Gruss A. 2010. Two coregulated efflux transporters modulate intracellular heme and protoporphyrin IX availability in *Streptococcus agalactiae*. PLoS Pathog 6:e1000860. https://doi.org/10.1371/journal.ppat.1000860.
17. Knippel RJ, Zackular JP, Moore JL, Celis AI, Weiss A, Washington MK, DuBois JL, Caprioli RM, Skaar EP. 2018. Heme sensing and detoxification by HatRT contributes to pathogenesis during *Clostridium difficile* infection. PLoS Pathog 14:e1007486. https://doi.org/10.1371/journal.ppat.1007486.
18. Torres VJ, Stauff DL, Pishchany G, Bezbradica JS, Gordy LE, Iturregui J, Anderson KL, Dunman PM, Joyce S, Skaar EP. 2007. A *Staphylococcus aureus* regulatory system that responds to host heme and modulates virulence. Cell Host Microbe 1:109–119. https://doi.org/10.1016/j.chom.2007.03.001.
19. Lechardeur D, Cesselin B, Liebl U, Vos MH, Fernandez A, Brun C, Gruss A, Gaudu P. 2012. Discovery of an intracellular heme-binding protein, HrtR, that controls heme-efflux by the conserved HrtB HrtA transporter in *Lactococcus lactis*. J Biol Chem 287:4752–4758. https://doi.org/10.1074/jbc.M111.297531.
20. Stauff DL, Skaar EP. 2009. *Bacillus anthracis* HssRS signalling to HrtAB regulates haem resistance during infection. Mol Microbiol 72:763–778. https://doi.org/10.1111/j.1365-2958.2009.06684.x.
21. Stauff DL, Skaar EP. 2009. The heme sensor system of *Staphylococcus aureus*. Contrib Microbiol 16:120–135. https://doi.org/10.1159/000219376.
22. Stauff DL, Torres VJ, Skaar EP. 2007. Signaling and DNA-binding activities of the Staphylococcus aureus HssR-HssS two-component system required for heme sensing. J Biol Chem 282:26111–26121. https://doi.org/10.1074/jbc.M703797200.
23. Joubert L, Derre-Bobillot A, Gaudu P, Gruss A, Lechardeur D. 2014. HrtBA and menaquinones control haem homeostasis in *Lactococcus lactis*. Mol Microbiol 93:823–833. https://doi.org/10.1111/mmi.12705.
24. Beavers WN, Monteith AJ, Amarnath V, Mernaugh RL, Roberts LJ, II, Chazin WJ, Davies SS, Skaar EP. 2019. Arachidonic acid kills Staphylococcus aureus through a lipid peroxidation mechanism. mBio 10:e01333-19. https://doi.org/10.1128/mBio.01333-19.
25. Ramos J, Martinez-Bueno M, Molina-Henares A, Teran W, Watanabe K, Zhang X, Gallegos M, Brennan R, Tobes R. 2005. The TetR family of transcriptional repressors. Microbiol Mol Biol Rev 69:326–356. https://doi.org/10.1128/MMBR.69.2.326-356.2005.
26. Routh M, Su C-C, Zhang Q, Yu E. 2009. Structures of the AcrR and CmeR: insight into the mechanisms of transcriptional repression and multi-drug recognition in the TetR family of regulators in the TetR family of regulators. Biochim Biophys Acta 1794:844–851. https://doi.org/10.1016/j.bbapap.2008.12.001.
27. Kumar R, Lovell S, Matsumura H, Battaile KP, Moenne-Loccoz P, Rivera M. 2013. The hemophore HasA from Yersinia pestis (HasAyp) coordinates hemin with a single residue, Tyr75, and with minimal conformational change. Biochemistry 52:2705–2707. https://doi.org/10.1021/bi400280z.
28. Aki Y, Nagai M, Nagai Y, Imai K, Aki M, Sato A, Kubo M, Nagatomo S, Kitagawa T. 2010. Differences in coordination states of substituted tyrosine residues and quaternary structures among hemoglobin M probed by resonance Raman spectroscopy. J Biol Inorg Chem 15:147–158. https://doi.org/10.1007/s00775-009-0579-4.
29. Halpern D, Gruss A. 2015. A sensitive bacterial-growth-based test reveals how intestinal Bacteroides meet their porphyrin requirement. BMC Microbiol 15:282. https://doi.org/10.1186/s12866-015-0616-0.
30. Mimee M, Nadeau P, Hayward A, Carim S, Flanagan S, Jerger L, Collins J, McDonnell S, Swartwout R, Citorik RJ, Bulovic V, Langer R, Traverso G, Chandrakasan AP, Lu TK. 2018. An ingestible bacterial-electronic system to monitor gastrointestinal health. Science 360:915–918. https://doi.org/10.1126/science.aas9315.
31. Fiorito V, Forni M, Silengo L, Altruda F, Tolosano E. 2015. Crucial role of FLVCR1a in the maintenance of intestinal heme homeostasis. Antioxid Redox Signal 23:1410–1423. https://doi.org/10.1089/ars.2014.6216.
32. Rockey DC. 2010. Occult and obscure gastrointestinal bleeding: causes and clinical management. Nat Rev Gastroenterol Hepatol 7:265–279. https://doi.org/10.1038/nrgastro.2010.42.
33. Seth EC, Taga ME. 2014. Nutrient cross-feeding in the microbial world. Front Microbiol 5:350. https://doi.org/10.3389/fmicb.2014.00350.
34. Fiore E, Van Tyne D, Gilmore MS. 2019. Pathogenicity of enterococci. Microbiol Spectr 7(4). https://doi.org/10.1128/microbiolspec.GPP3-0053-2018.
35. Brewitz HH, Hagelueken G, Imhof D. 2017. Structural and functional diversity of transient heme binding to bacterial proteins. Biochim Biophys Acta Gen Subj 1861:683–697. https://doi.org/10.1016/j.bbagen.2016.12.021.
36. Maresso AW, Schneewind O. 2006. Iron acquisition and transport in *Staphylococcus aureus*. Biometals 19:193–203. https://doi.org/10.1007/s10534-005-4863-7.
37. Price EE, Boyd JM. 2020. Genetic regulation of metal ion homeostasis in *Staphylococcus aureus*. Trends Microbiol 28:821−831. https://doi.org/10.1016/j.tim.2020.04.004.
38. Orelle C, Mathieu K, Jault JM. 2019. Multidrug ABC transporters in bacteria. Res Microbiol 170:381–391. https://doi.org/10.1016/j.resmic.2019.06.001.
39. Yang HB, Hou WT, Cheng MT, Jiang YL, Chen Y, Zhou CZ. 2018. Structure of a MacAB-like efflux pump from *Streptococcus pneumoniae*. Nat Commun 9:196. https://doi.org/10.1038/s41467-017-02741-4.
40. Sharom FJ. 2006. Shedding light on drug transport: structure and function of the P-glycoprotein multidrug transporter (ABCB1). Biochem Cell Biol 84:979–992. https://doi.org/10.1139/o06-199.
41. Bull-Henry K, Al-Kawas FH. 2013. Evaluation of occult gastrointestinal bleeding. Am Fam Physician 87:430–436.
42. Zeng MY, Inohara N, Nunez G. 2017. Mechanisms of inflammation-driven bacterial dysbiosis in the gut. Mucosal Immunol 10:18–26. https://doi.org/10.1038/mi.2016.75.
43. Berry EA, Trumpower BL. 1987. Simultaneous determination of hemes a, b, and c from pyridine hemochrome spectra. Anal Biochem 161:1–15. https://doi.org/10.1016/0003-2697(87)90643-9.
44. Lechardeur D, Fernandez A, Robert B, Gaudu P, Trieu-Cuot P, Lamberet G, Gruss A. 2010. The 2-Cys peroxiredoxin alkyl hydroperoxide reductase c binds heme and participates in its intracellular availability in *Streptococcus agalactiae*. J Biol Chem 285:16032–16041. https://doi.org/10.1074/jbc.M109.024505.
45. Wolff SP. 1994. Ferrous iron oxidation in presence of ferric ion indicator xylenol orange for measurement of hydroperoxides. Methods Enzymol 233:182−189. https://doi.org/10.1016/S0076-6879(94)33021-2.